

PLANAR ANTENNA ARRAYS ON LTCC-MULTILAYER TECHNOLOGY

S.Holzwarth, J.Kassner, R.Kulke, D.Heberling

IMST GmbH, Germany, e-mail: holzwarth@imst.de

ABSTRACT

The market of RF and microwave circuits and modules is nowadays facing a constant demand for cost reduction, high integration and high performance. As a result, LTCC (Low Temperature Co-fired Ceramics) multilayer technology is becoming more and more popular for the production of highly integrated, complex multilayer modules and circuits. This technology is appreciated for its flexibility in realising an arbitrary number of layers with easy-to-integrate circuit components like via-holes, thick film resistors, cavity-buried or top-mounted SMT components, or even chip devices. Circuits on different layers can be connected with the help of via-holes or field-coupled transitions, and be shielded from each other by ground meshes between the layers.

For the mobile telecommunication frequency range up to the L-Band, the manufacturing tolerances and typical design rule limitations of the LTCC technology are generally not posing serious problems. For the range of the K- or Ka-Band, however, these aspects must be considered more carefully, because the tolerances become more critical with respect to the wavelength. Since the line loss is known to increase with higher frequencies, feeder losses have also to be considered more carefully in the design of antenna arrays. Yet, the demand for high integration is especially increasing for these frequency bands. The integration of antenna elements with active front-end components, for example, reduces losses in the distribution network, thus increasing both the sensitivity of the receiver and the efficiency of the power supply of the transmitter. An emerging demand for active and smart antennas mirrors this trend. It is therefore worthwhile to investigate LTCC antenna and circuit design for such applications.

LTCC materials typically possess a high dielectric constant. On one hand, this helps to reduce the circuit size, but on the other hand also reduces the bandwidth and efficiency of planar antennas, thus making the design more difficult and therefore more challenging.

This paper will present the design and prototyping of different 24.125 GHz LTCC aperture-coupled patch antenna arrays for ISM-band applications. As shown in Figure 1, the feeding network of the antenna arrays has been designed either using T-junctions or Wilkinson-dividers. To prototype the latter, integration of thick film or SMT resistors and LTCC is necessary. Simulation analysis as well as thorough measurement characterisation of the antennas performance will show chances and limits of LTCC-technology in the design of planar antenna arrays.

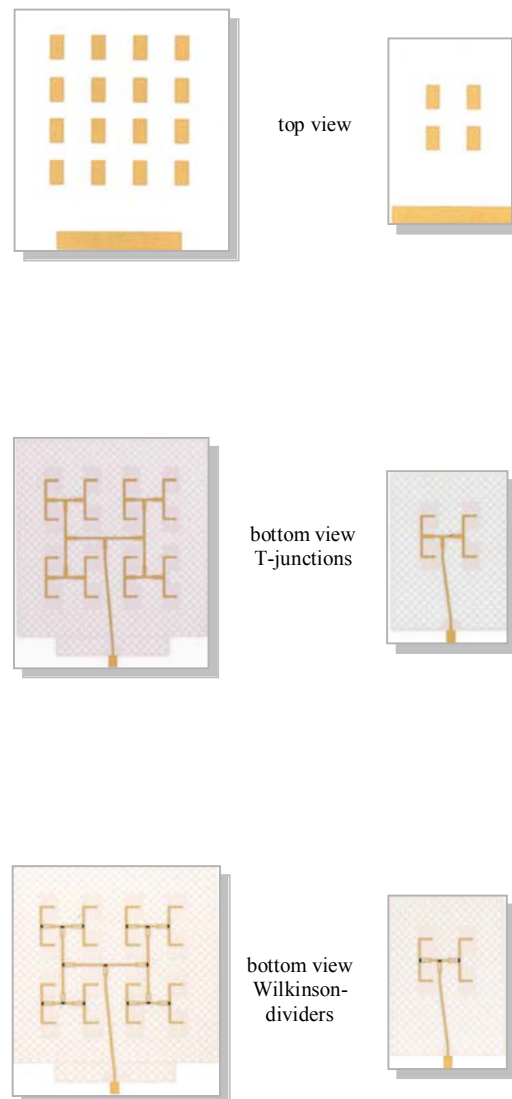


Figure 1: LTCC antenna prototypes: 2x2 and 4x4 array.

DESIGN

Layer structure

The LTCC multilayer structure discussed in this paper consists of four ceramic tapes of equal thickness (0.185 mm). Figure 2 shows a cross section of the layer structure. It is useful to design the feeding network on a thin substrate, thus minimising radiation of the feeding network, and to use a thick substrate for the patch elements to achieve good antenna radiation and bandwidth. Therefore, one single ceramic tape is used to carry the microstrip feeding line, whereas the patch elements, which are located on top of the multilayer structure, are using three ceramic tapes. After the ceramic laminating and sintering process, these tapes form one homogeneous medium.

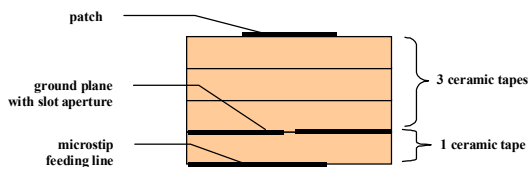


Figure 2: Layer structure of the aperture coupled patch antenna element.

Material properties

Prior to the design of the antenna structures, measurements of test structures have been done to analyse the material properties of the LTCC material used (FERRO A6-M). A specific resistivity (relative to the resistivity of gold) of 1.6 and a metal roughness of 0.4 μm was derived from these measurements. LTCC-Technology data sheets [1] state the dissipation factor of the FERRO A6-M ceramic to be 0.0012 at 5 GHz. For the operating frequency of 24.125 GHz, a dissipation factor of 0.002 has been assumed. Table 1 summarises the material characteristics which, in the following, have been used for the calculations of line loss, efficiency and gain.

ϵ_r	$\tan\delta$	ρ/ρ_{Au}
5.9	0.002	1.6

Table 1: Material parameters of the FERRO A6-M ceramic with thick film conductor at 24.125 GHz.

ϵ_r : dielectric constant

$\tan\delta$: dissipation factor

ρ/ρ_{Au} : specific resistivity /specific resistivity of gold

Determination of expected gain

It has widely been reported in literature that the gain of antenna arrays is limited due to feeder losses [2]. Beyond a certain aperture size, the gain will reduce. This critical size is mainly dependent on the feeder topology and the material properties. Thus, prior to the design of antenna arrays on the LTCC material, it is worthwhile to estimate the expected gain based on the planned feeder topology and the array size.

In a first step, the line loss of a 50 Ω microstrip feeding line has been calculated. For the calculations, a 2.5 D simulation tool (ENSEMBLE) has been used. The simulation model assumes all substrate and ground planes to be of infinite size. The thickness of the conductor and the roughness of the metal are not considered. Table 2 shows the calculated dielectric, metallic and total line loss per cm at the operating frequency of 24.125 GHz.

In a second step, the directivity and gain of a single aperture coupled patch element has been calculated considering metallic respectively dielectric losses. The results are shown in Table 3.

Z_0 [Ω]	α_d [dB/cm]	α_m [dB/cm]	α_t [dB/cm]
50	0.1	0.2	0.3

Table 2: Calculated dielectric, metallic and total line loss for a microstrip feeding line at 24.125 GHz.

Z_0 : Impedance of the microstrip feeding line

α_d : dielectric line loss per cm

α_m : metallic line loss per cm

α_t : total line loss per cm

D [dBi]	G_d [dBi]	G_m [dBi]	G_t [dBi]
4.8	4.65	4.75	4.6

Table 3: Calculated directivity and gain of a single aperture-coupled patch element considering metallic resp. dielectric losses.

D : Directivity

G_d : Gain considering dielectric losses

G_m : Gain considering metallic losses

G_t : Gain considering both losses

Finally, the expected gain has been determined by adding up the element gain [dBi] and the array factor [dB], and subtracting the line losses [dB] of the feeding network. The estimation considers square antenna arrays consisting of $2^n \times 2^n$ elements ($n = 1, 2, 3, \dots$) with an element distance of half a free space wavelength. As depicted in Figure 1, a corporate feeding network is used to excite the antenna elements with equal amplitude and phase. For the configuration investigated in this paper, the port of the antenna is located at the edge of the substrate. As shown in Figure 3, this edge-fed solution considerably prolongs the length of the feeding network in comparison to a centre-fed solution. Therefore, the efficiency of this antenna array is lower than that of a similar centre-fed solution. Since, for some applications, a centre-fed configuration might be conceivable, both cases are considered and depicted in Figure 4.

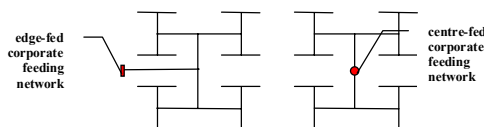


Figure 3: Edge-fed and centre-fed corporate feeding networks for 4x4 antenna arrays.

The straight lines in the diagram indicate the efficiency curves of 100% (ideal gain curve) and 50%. The critical array size is about 32×32 elements (ca. $20 \times 20 \text{ cm}^2$). The typical size of ceramic wafers is about $15 \times 15 \text{ cm}^2$ ($6 \times 6 \text{ in}^2$). This means that the maximum size of the antenna arrays will rather be limited by the size of the ceramic wafer than by the critical array size.

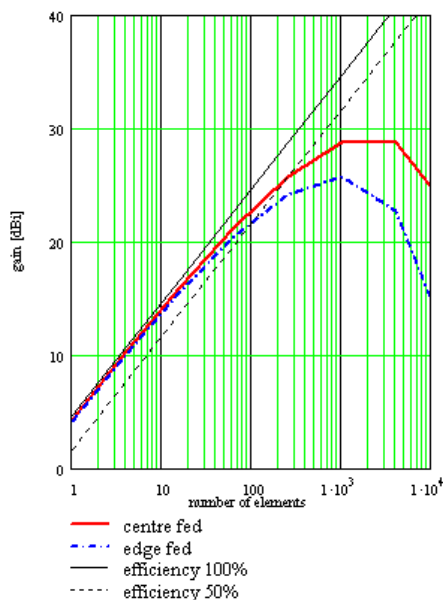


Figure 4: Estimation of expected gain vs. number of array elements on proposed antenna array structure.

Bandwidth

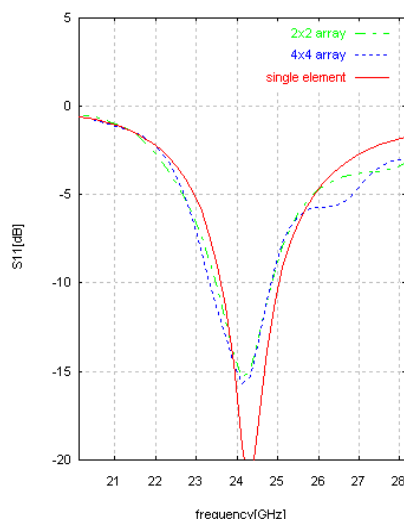


Figure 5: Calculated reflection coefficient of a single element, 2×2 and 4×4 antenna array with T-junctions.

The rather high dielectric constant of the LTCC material makes the design of antennas more critical concerning bandwidth. Figure 5 shows the calculated reflection

coefficient of a single aperture coupled patch antenna element together with results for a 2×2 and 4×4 antenna array. A 10 dB bandwidth of about 5% can be stated, which is sufficient for ISM-band applications.

PROTOTYPING

Wilkinson dividers

The antenna arrays presented here differ by their feeding network. As shown in Figure 1, for one type of antenna arrays, T-junctions are used as power dividers, whereas for the other type, Wilkinson-dividers are applied. To prototype the latter, the integration of thick film or SMT resistors and LTCC is necessary. There are different manufacturing techniques to realise thick film resistors. One way is to fire the thick film paste together with the ceramic sintering process (cofired thick film resistors), the other way is to fire the thick film paste in an additional manufacturing process after sintering the ceramics (postfired thick film resistors). Different prototypes have been realised using both techniques. The resistor values of the thick film resistor pastes are known to differ about 30% from the nominal value. For reasons of comparison, some prototypes have also been build up using SMT resistors.

Meshed ground plane

Since the manufacturing process does not allow solid ground planes between ceramic tapes, the inner metal layer is realised as a meshed ground plane.

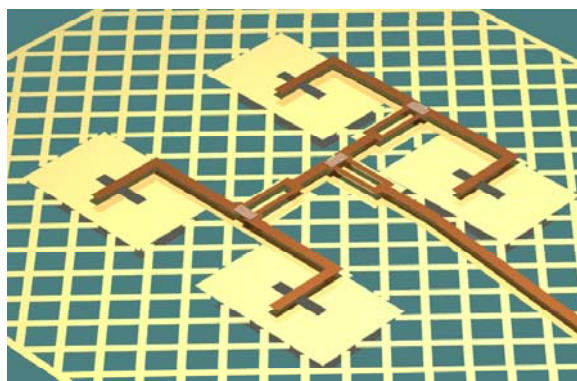


Figure 6: Feeding network and meshed ground plane of a 2×2 antenna array with Wilkinson-dividers.

Figure 6 shows the 3D-layout model of the feeding network and the meshed ground plane of a 2×2 antenna array with Wilkinson-dividers. The ground plane located directly beneath the microstrip feeding network and the patch elements is solid, thus avoiding additional line losses as well as a change in the impedance of the microwave feeding network and the patch elements. The complete 2×2 and 4×4 antenna arrays have been calculated using the $2.5 D$ simulation tool ENSEMBLE. Due to the complexity of the mesh, the meshed ground plane could not be taken into account. Instead, the ground plane has been modelled solid and infinitely extended.

MEASUREMENTS

Reflection coefficient

The reflection coefficient of all antenna prototypes has been measured with the help of a coaxial connector mounted at the edge of the substrate. Although the SMA-connectors used are actually not specified for the operating frequency band, the reflection coefficient was found to be better than -10 dB for all antenna prototypes at the operating frequency of 24.125 GHz .

Far field measurements

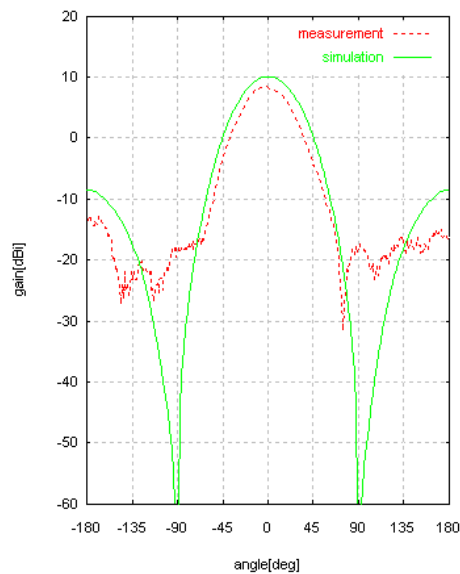


Figure 7: Calculated and measured gain function of a 2×2 antenna array with T-junctions (H-plane).

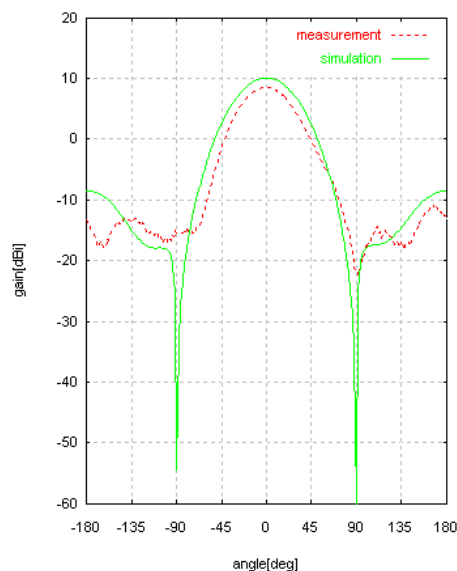


Figure 8: Calculated and measured gain function of a 2×2 antenna array with T-junctions (E-plane).

Both the far field patterns and the gain of all antenna prototypes have been measured. Figure 7 to Figure 10 show the measured results for the 2×2 and 4×4 antenna array prototypes with T-junctions in comparison with the simulation results. The measured far field patterns of the antenna arrays are in good agreement with the calculated results. The main deviations naturally occur in the region around $\pm 90^\circ$, since the simulation models are not taking into account the finite size of the ground plane. Some asymmetry in the measurement results can be observed in the E-plane of the antenna arrays. Possible reasons for this effect can be amplitude and phase errors, which might be caused by effects of the meshed ground plane.

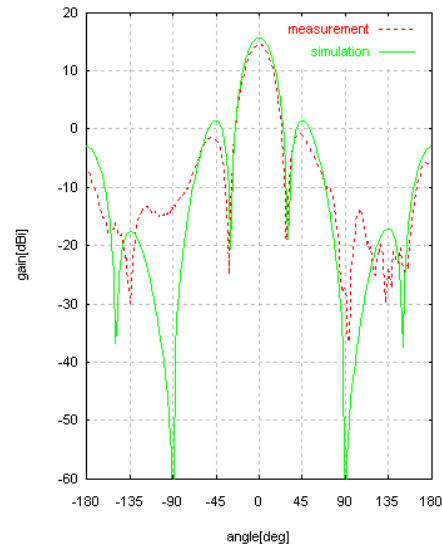


Figure 9: Calculated and measured gain function of a 4×4 antenna array with T-junctions (H-plane).

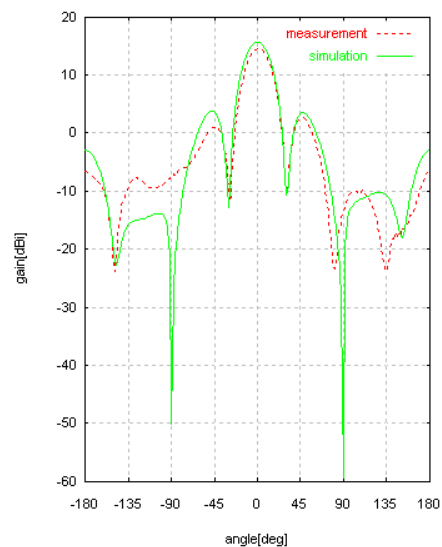


Figure 10: Calculated and measured gain function of a 4×4 antenna array with T-junctions (E-plane).

Since the simulation models of the complete antenna arrays include material losses, not only the far field patterns but also the calculated gain can be compared with the measurement results. A good agreement can be stated for the 4x4 antenna array. The gain of the 2x2 array, having smaller directivity, is stronger influenced by the effect of the finite ground plane. The deviations between calculated and measured gain of the 2x2 array might result from this effect.

Comparison of the prototypes

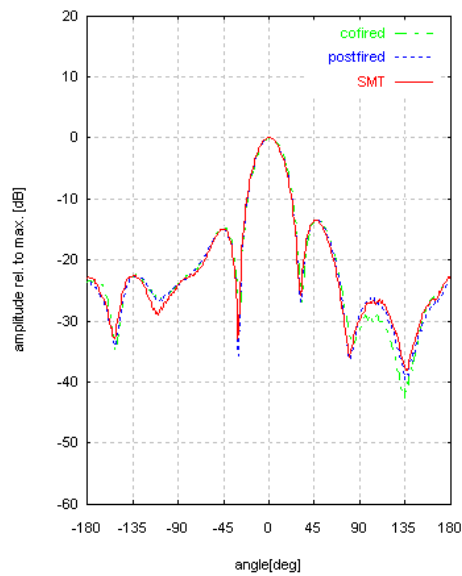


Figure 11: Measured far field patterns of different 4x4 antenna array prototypes (E-plane).

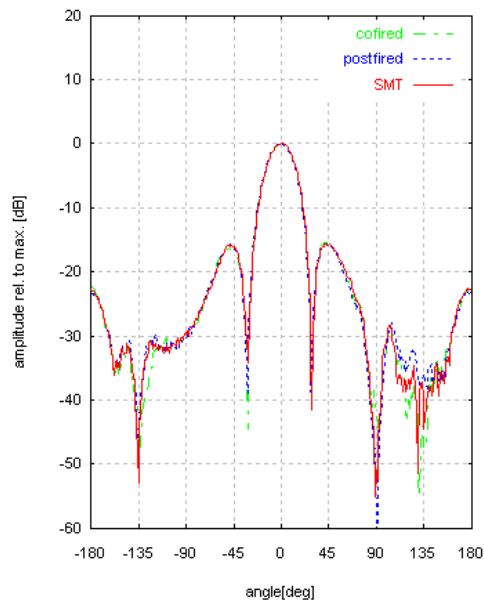


Figure 12: Measured far field patterns of different 4x4 antenna array prototypes (H-plane).

Figure 11 and Figure 12 show a comparison between the measurement results of the far field patterns of different 4x4 antenna array prototypes with Wilkinson-dividers. A very good reproducibility can be observed. This indicates that for the feeding network used, the deviations of the thick film resistor values from the nominal values hardly influence the performance of the antennas.

SUMMARY

This paper has presented the design and prototyping of different 24.125 GHz LTCC aperture-coupled patch antenna arrays for ISM-Band applications. Thorough analysis of material loss, gain and bandwidth shows the LTCC material used to be well suited for realising antenna arrays up to the typical ceramic wafer size of about $15 \times 15 \text{ cm}^2$ ($6 \times 6 \text{ in}^2$). Some aspects of the prototyping process like the implementation of meshed ground planes and the realisation of integrated thick film resistors have been discussed. Various measurements of far field patterns and gain have been presented and found to be in good agreement with the simulation results. Finally, the measurement results of different antenna prototypes show a very good reproducibility.

ACKNOWLEDGEMENT

The work of this paper is derived from the European BriteEuram III project RAMP ("Rapid Manufacture of Microwave and Power Modules" BE-97-4883). The antenna arrays discussed in this paper have been manufactured by SOREP-ERULEC, France.

LITERATURE

- [1] "LTCC for Radio Frequency Applications, Advanced RF system", Data sheet, SOREP ERULEC, Châteaubourg Cedex, 2000.
- [2] J.R. James, P.S. Hall: „Handbook of Microstrip Antennas“, Vol. 1, Peter Peregrinus Ltd., London, 1989